Differential sensitivity to temperature and evaporative demand in wheat relatives

Stéphane Leveau, Boris Parent, Serge Zaka, Pierre Martre

Sensitivities to temperature and evaporative demand in wheat relatives

Stéphane Leveau[1,2], Boris Parent[1], Serge Zaka[2] and Pierre Martre[1]

[1] LEPSE, Univ Montpellier, INRAE, Institut Agro, Montpellier, France; [2] ITK, Clapiers, France

stephane.leveau@inrae.fr /boris.parent@inrae.fr / serge.zaka@itk.fr / pierre.martre@inrae.fr

Authors for correspondence:

Dr. Boris Parent

Tel. : +33 499 613 183

Email: boris.parent@inrae.fr

Dr. Pierre Martre

Tel.: +33 499 612 958

Email: pierre.martre@inrae.fr

Highlight

Ploidy, phylogeny and breeding together structure the genetic variability of leaf growth and development and their sensitivities to temperature and evaporative demand in 12 wheat-related species and subspecies.

Abstract

There is potential sources of alleles and genes currently locked into wheat-related species that could be introduced into wheat breeding programs for current and future hot and dry climates. However, neither the intra- nor the inter-specific diversity of the responses of leaf growth and transpiration to temperature and evaporative demand have been investigated in a large diversity of wheat-related species. By analysing 12 groups of wheat-related sub-species, we questioned the n-dimensional structure of the genetic diversity for traits linked to plant vegetative structures and development, leaf expansion and transpiration together with their responses to "non-stressing" range of temperature and evaporative demand. In addition to provide new insight on how genome type, ploidy level, phylogeny and breeding pressure together structure this genetic diversity, this study provides new mathematical formalisms and the associated parameters of trait responses in the large genetic diversity of wheat-related species. This potentially allow crop models predicting the impact of this diversity on yield, and indicate potential sources of varietal improvement for modern wheat germplasms, through interspecific crosses.

Key words: evaporative demand, leaf expansion, leaf growth, genetic diversity, temperature, transpiration, vapour pressure deficit (VPD), wheat.

Short summary

There is potential sources of wheat improvement that are currently locked into wheat-related species. In order to allow crop models predicting the impact of this diversity under dry and hot climates, we (i) analyse 12 wheat-related sub-species for their responses to temperature and evaporative demand, (ii) provide new mathematical formalisms and the associated parameters of such response traits. (iii)and question how genome type, ploidy level, phylogeny and breeding pressure together structure this genetic diversity.

Introduction

Cereal production is affected worldwide by high temperature, high evaporative demand and drought . The frequency of such events increases because of climate change , while agriculture is challenged by societal and policy requirements for a more sustainable and water-sparing agriculture. Developing new cultivars adapted to this dual context is not straightforward, knowing (i) the high diversity of climates and management practices in wheat-growing regions and (ii) that each genotypic trait can have positive effects on crop performance in one type of environment while being deleterious in another one .

A purely experimental approach cannot explore the effects on yield, plant resilience, or environmental balances of each combination of traits under all possible environmental scenarios. A combination of experimental and modelling approaches is required to define the best combinations of traits in a target environment , using models that predicts genotypic effects under various environmental scenarios . These models necessitate formalisms of specific responses to environmental constraints, adapted to a large genetic variability, together with associated trait/parameter values covering the range that breeders can meet within enlarged breeding pools .

This is not yet the case for the responses of wheat leaf expansion and transpiration to temperature and evaporative demand in crop growth models. However, for example, the control of transpiration under high evaporative demand can be the key if one aims at designing future cultivars that can produce “more crop per drop” . In wheat models, availability of efficient formalisms and parameter values differ largely between processes:

-The response of leaf expansion to temperature was found to be similar to that of plant development , at least in a “non stressing” range, in which processes are not durably affected, and reversible (Parent *et al.*, 2010). In such ranges of temperature, which are not considered as “heat or cold stresses”, development responses to temperature are well-formalized and parameter values are determined in most cultivated species. Indeed, these responses are the base of the calculation of thermal time, a central concept of most process-based models.) have indicated a very low variability of this response within each species they studied, while they found a wider variability between species. However, up to now, the variability of temperature responses and the possibility of seeking new alleles controlling temperature responses between closely-related species such as wheat-related species has not been documented.

-While evaporative demand has been found as largely affecting leaf expansion rate (LER) in several species (e.g. , very little is known about how wheat growth is affected and whether significant genetic variability exist in wheat or wheat-related species. This is probably due to the fact

that temperature and vapour pressure deficit (VPD) are difficult to dissociate in natural environments. There is an urgent need to characterize these responses, both for the accuracy of model predictions and to inform breeders on the availability (or not) of an associated genetic variability in wheat.

-The response of transpiration to VPD has been studied in several crops including wheat . In wheat, breeders have indirectly selected genotypes that present a limitation in hydraulic conductance , allowing to decrease transpiration at high VPD. However, we do not know if the reported range of response represents a large part of the genetic variability in wheat related species (genus *Triticum* and *Aegilops)*, or if genetic variability has been lost during wheat domestication and breeding.

Wheat-related species form a large family (> 300 species and subspecies), including wild and cultivated species domesticated over 10,000 years, three subgenomes (A, B and D), and three levels of ploidy (diploid: A^u, A^m, B and D genome; tetraploids: AB subgenomes; hexaploids: ABD subgenomes). Polyploid *Triticum* species originated by natural hybridization events between *Triticum* and *Aegilops* (Fig. 1) . Bread wheat (*T. aestivum*) represents 95% of global wheat production and is grown in a very wide range of latitude and altitude . Durum wheat (*T. turgidum* subsp. *durum*) is mainly grown under Mediterranean-type climates. Other wheat species are grown more marginally, such as spelt (*T. aestivum subsp. spelta*), einkorn (*T. monococcum subsp. monococcum*), or emmer wheat (*T. turgidum subsp. dicoccum*).

Because of the availability of wild wheat-related species, there is a large reservoir of alleles and genes currently locked into wild backgrounds that can be introduced into wheat breeding programs through interspecific crosses. For example, bread wheat emerged from the natural hybridization between wild goatgrass (*Ae. tauschii*) and a cultivated tetraploid wheat (*T. turgidum* subsp. *dicocccum*, a progenitor of modern durum wheat). However, the genetic diversities of *T. turgidum* and *Ae. tauschii* are not fully represented in *T. aestivum,* probably because it has evolved from only few hybridization events. Introducing genes from wheat-relative species can therefore increase the genetic diversity of modern germplasms (Gorafi et al., 2018), for example by synthetic crosses between tetraploid wheats and *Ae. Tauschii* and between *T. aestivum and T. turgidum* .

The higher tolerance of durum wheat to heat and drought stress compared with bread wheat is still debated . Indeed, inter-comparisons were generally performed based on yield only or yield components , and our knowledge regarding the differences in plant responses to abiotic constraints is still limited . Physiological responses at fine scales can be very different from macroscopic

responses, which are the emerging properties of numerous underlying processes, integrated over the whole growth cycle .

Such inter-specific genetic variability can originate from genes or alleles currently locked in wild species but also from ploidy itself. Traits expressed in wild diploids may not predict the traits in progeny of higher ploidy after synthetic hybridizations. Indeed, ploidy itself can provide agronomic advantages or disadvantages , for example by conferring resistance to biotic and abiotic stresses .

In this study, we analysed 12 groups of wheat-related sub-species (five accessions each) for traits linked to vegetative structure and development, leaf expansion and transpiration together with their responses to ranges of "non-stressing" temperature and evaporative demand during the vegetative phase. We used an original experimental protocol and selected model formalisms adapted to this broad genetic diversity, in order to compare the intra-and inter-specific diversities. We concluded that the genome type, ploidy level and phylogeny together structure the genetic diversity, and that breeding pressure may have indirectly pushed these traits in specific directions. Overall, in addition to provide new formalisms of trait responses together with model parameters to be included in process-based models for large-scale simulations, this study indicates potential sources of varietal improvement for modern wheat germplasms, currently locked into related species.

Materials and Methods

Plant Material

We analysed 12 wheat-related species (Fig. 1) and selected five accessions per species in order to maximise the genetic diversity in each species (Supporting Information Tables S1 and S2). This set of species includes wild and cultivated species with different levels of ploidy:

- Wild diploid species: *T. monocuccum* subsp. *boeticumm* (A^m genome), *T. urartu* (A^u genome), *Ae. tauschii* (D genome) and *Ae. speltoides* (S genome, related to species belonging to *Ae.* sect. *sitopsis* from which B-genome originated).
- Cultivated diploid species: einkorn wheat (*T. monococcum* subsp. *monococcum*, A^m genome) domesticated from *T. monocuccum* subsp. *Boeticumm.*
- Wild tetraploid species: wild emmer wheat *T. turgidum* subsp. *dicoccoides* (AB genome) coming from the natural hybridization event between *T. uratu* and an unknown species belonging to *Aegilops* sect. *sitopsis.*
- Cultivated tetraploid species: cultivated emmer wheat (*T. turgidum* subsp. *dicoccum*, AB genome) domesticated from wild emmer wheat, rivet wheat (or poulard wheat, *T. turgidum*

subsp. *turgidum*, AB genome), which evolved from *T. turgidum* subsp. *dicoccum*, and durum wheat (*T. turgidum* subsp. *durum*, AB genome), which was domesticated from *T. turgidum* subsp. *dicoccum*, which we separated in two groups: landraces from before the green revolution and elite cultivars released after the green revolution.

- Cultivated hexaploid wheats: spelt wheat (*T. aestivum* subsp. *spelta)* and bread wheat (*T. aestivum* subsp. *aestivum)* coming from natural hybridization events between *T. turgidum* subsp. *dicoccum* and *Ae. tauschii.*

Plant growth conditions

All experiments were conducted in the plant phenotyping platform Phenodyn, part of M3P plant phenotyping platforms (M3P, Montpellier, France, https://www6.montpellier.inrae.fr/lepse_eng/M3P). Briefly, this platform is set-up with balances to monitor plant transpiration, displacement transducers to monitor leaf expansion, a set of climatic sensors and automatic drip feed systems. Air temperature, relative humidity, and PPFD were measured at the plant level and stored every 15 min in a data logger (CR10X, Campbell Scientific LTD, Leicestershire, UK). The temperature of the leaf meristematic (growth) zone was measured with thermocouples inserted vertically inside the sheath of leaf 5 of three to six plants, and used to calculate meristem-to-air VPD. VPD was controlled based on measurements of relative humidity and temperature.

Seeds were imbibed for 24 h at 4°C on water-saturated filter papers in Petri dishes, then placed at room temperature for 24 h and put back at 4°C for 48 h. Six germinated seeds were planted in 9-L plastic pots (id 20 cm) filled with a 40:60 (v:v) mixture of clay and organic compost and then thinned to three plants per pot when the third leaf emerged. A total of three pots (nine plants) per accession were sown, together with four pots with non-transpiring artificial plants mimicking real plants used to calculate evaporation from soil surface. Sowing was spread over eleven weeks in order to stagger measurements in the growth chambers. A fully randomized design was used. Pots with less than three emerged plant were sown again during the 12th week.

Plants were grown for three weeks in a growth chamber where temperature and VPD were controlled at 20.6 ± 2.6°C / 16.3 ± 1.9°C (day/night) and 1.4 ± 0.4 kPa / 0.9 ± 0.3 kPa (day/night), respectively. PPFD at plant level averaged 300 µmol s^{-1} m^{-2} during the 12-h photoperiod. Plants were watered daily to maintain the soil water potential above -0.05 MPa. Three weeks after plant emergence, two pots (six plants) of each accession were transferred to another growth chamber and were subjected to various temperature and VPD conditions (scenario 1) during a 4-days period and

one pot (three plants) underwent a second scenario (scenario 2), with more extreme temperatures (Supplementary Information Fig. S1). This period of measurement was selected because it corresponded to the appearance of leaf-5 in all genotypes, for comparing absolute values of leaf elongation rate, and because internode elongation had not started yet. Indeed, the automatic measurement of leaf elongation with displacement transducers does not make possible to discriminate elongations of internode and leaves at latter plant stages. In both scenarios, plants were harvested at the end of the 4-days period. We used two scenarios applied in different growth chamber and on different plants to compare the response of LER to temperature on plants at similar development stages on the full range of target temperatures.

In scenario 1, each night, plants were subjected to two air temperature values: a reference temperature of 20°C during 6 h, and another temperature value (the target temperature; either 12°C, 16°C, 24°C, or 28°C) during the following 6 h. Each night, the lowest temperature (between the two temperatures) was applied first. During the first three days, during daily hours, plants were subjected to two VPD values: a 6-h period with a reference VPD of 1.3 kPa and a 6-h period with the target VPD value (either 0.5, 2.5, or 3.0 kPa). Each day, the lowest VPD value was applied first. The daytime air temperature was set in such a way that the target air VPD values were attainable (20°C for VPD at 0.5 kPa; 26°C at 2.5 kPa; 28°C at 3.0 kPa), but in all cases, temperature was similar for both the reference and the tested VPD. The fourth day, air temperature and VPD were maintained at 20°C and 1.3 kPa, respectively.

In scenario 2, a protocol similar to that of scenario 1 was applied but with more extreme temperatures and VPD values. The target air-temperature values were 4°C, 8°C, 32°C, and 36°C and the target air VPD values were 0.3, 2.5 and 4 kPa. Because VPD was not stable enough in these conditions, in latter analyses, data of plant responses to night temperature were used but not data measured during the light period. As in scenario 1, the fourth day temperature was maintained at 20°C and VPD at 1.3 kPa.

Response of leaf elongation rate to temperature

The youngest growing leaf (leaf 4 or 5 during the first night and leaf 5 or 6 for the last day of measurements) was attached to a rotary displacement transducer (601–1045 Full 360 Smart Position Sensor; Spectrol Electronics, Ltd, Wiltshire, England). Leaf elongation was transmitted to the sensor via a pulley attached to it, which carried a thread attached to the leaf tip and to a 10 g counterweight. Leaf elongation was recorded on a data logger every 15 min.

The response of leaf elongation rate (LER) to leaf growth zone temperature was calculated from both temperature scenarios during the night period to avoid confounding effects of temperature and evaporative demand. In all cases, LER stabilized within 2 h after the beginning of the night period or of the change in temperature (Fig. 2, checked on all plants). LER was averaged over the last 4 h of each period. In wheat, LER of a given leaf is not steady and depends on leaf rank. Therefore, in order to compare LER of leaves of different lengths (relative to their final length) and rank, LER at the tested temperature was normalized by LER at the reference temperature (20°C) measured during the same night. To determine the cardinal temperatures of normalized LER, data were fitted with a 3-parameter segmented linear function equation constrained to be equal to unit at the reference temperature:

$$f(T) = \begin{cases} \frac{(T - T_{\min})}{(T_{\text{ref}} - T_{\min})} & , \ T < T_{\text{opt}} \\ \frac{(T - T_{\max})(T_{\text{opt}} - T_{\min})}{(T_{\text{ref}} - T_{\min})(T_{\text{opt}} - T_{\max})} & , \ T \geq T_{\text{opt}} \end{cases} \quad \text{Eqn 1}$$

where T (°C) is the temperature of the leaf meristematic-zone, T_{ref} (°C) is the reference temperature at which $f(T)$ is equal to unit, T_{min} (°C) is the base temperature at which normalized LER equals zero, T_{opt} (°C) is the temperature at which normalized LER is maximal, and T_{max} (°C) is the supra-optimal temperature at which normalized LER stops (Table 1). Eqn (1) was compared with a beta function and an Arrhenius-type function . Regression were performed with the BFGS method of the *optim* function (software R; . The goodness of fit of the three equations was evaluated with the root mean squared error and models were compared with the Akaike information criterion and the Bayesian information criterion .

Responses of leaf elongation rate and transpiration to vapour pressure deficit

The response of LER and transpiration to leaf-air VPD was calculated during the day in scenario 1 only. LER was measured as described above. Transpiration rate (TR) was calculated from the weight loss of each pot divided by the total leaf (sheath + blade) area. Direct evaporation from the soil was estimated by measuring the weight loss of pots carrying plastic plants, which were water to maintain a soil water potential similar to that of the studied pots. The weight of the pots was averaged and stored every 15 min.

LER of the youngest growing leaf measured at the 15 min time-step was first expressed with units of thermal time in order to remove the effects of temperature. It was then averaged for the period of

stabilized VPD (last 4 h of the 6-h period) and was then normalized by the average TR during 4 h at the reference VPD, removing effects of plant size and leaf area. Normalized LER and TR data were then fitted with a linear model, constrained to unit at the reference VPD, so that only one parameter described each response, the sensitivities of LER (sLER, kPa^{-1}) and TR (sTR, kPa^{-1}) to VPD.

Traits linked to rates of development, leaf expansion and transpiration

Progress of plant development one the main stem, was determined from leaf stage (LS; adapted from :

$$\mathrm{LS} = n + \frac{l}{L} \quad \text{Eqn 2}$$

where *n* is the number of ligulated leaf, and *l* and *L* are the exposed and final lengths of the blade of leaf *n* + 1, respectively. The exposed length of a leaf was measured with a ruler as the distance from leaf tip to the upper collar of the sheath tube. LS was determined on all plants of scenario 1 from the day before to the last day of LER measurements. The rate of leaf appearance (LAR, leaf $°Cd^{-1}$; inverse of phyllochron) was calculated as the slope of the relationship between LS and thermal time (base 0°C).

Because LER of leaf 5 was measured during at least one night for all accessions, the absolute LER of all accessions was compared based on LER of leaf 5 (LERm, mm h^{-1}) measured at 20°C, 2 to 3 days after leaf appearance (i.e. when LER was at its maximum value). TR at 20°C and 1.3 kPa was calculated as the average of TR measured each of the four nights during a 6-h period. At the end of the 4-days period, the whole-plant leaf area was measured (see below). TR per unit of leaf area (TR, g cm^{-2} h^{-1}) was calculated by first removing evaporation of pots with plastic plants and then dividing it by the whole-plant leaf area.

Traits linked to plant structure

All plant structural traits were measured after the fourth day of LER and transpiration measurements. Total number of leaves per plant (TL, leaf $plant^{-1}$) was counted. The leaf blades and sheaths of the main stem and tillers were then separated and their length, width, and surface area were measured with an electronic planimeter (LI-3100C, Li-Core Inc., Lincoln, NE, USA). Several traits linked to plant structure were calculated from these measurements. The total leaf area per plant was calculated (LAT, cm^2 $plant^{-1}$). The length-to-width ratio (rlw2, dimensionless) and surface area (LA2, cm^2 $plant^{-1}$) of the blade of main stem leaf 2 were calculated as proxies of plant early vigour . The slope of the relationship between main stem individual leaf blade surface area and leaf rank

normalized by the surface area of the blade of leaf 2 (sLAK, dimensionless) and the ratio of leaf blade to total leaf (sheath + blade) surface area (rLA, dimensionless) were also calculated.

The main stem leaf blades and sheaths of each plant were pooled and oven dried at 85°C until constant mass. The dry mass of the samples was measured and specific leaf mass (MLA, g DM cm^{-2} leaf) was calculated by dividing total plant dry mass by TL. Samples were then milled and their total N concentration (N mass per unit dry mass) was determined with the Dumas combustion method (Association of Official Agricultural Chemists method no. 7.024) using a FlashEA 1112 N/Protein Analyzer (Thermo Electron) and the mass of N per plant was calculated (PN, g N $plant^{-1}$). Specific leaf N mass (SLN, g N m^{-2} leaf) was calculated by dividing PN by TL.

Data analyses

All data analyses were carried out with the statistical program software R . Analyses of variance on each variable were performed with the function *aov*, considering species as factors and genotypes as replicates. Confidence intervals of differences between means of each couple of species were calculated using a Tukey test (R function *TukeyHSD*) and significance of these differences were calculated with function *HSD.test* with α =0.05

The procedure for building correlograms included the following step: (i) normality Shapiro-Wilk test; (ii) calculation of Spearman correlations; and (iii) calculation of *q*-values (*P*-value corrected for false discovery rate). Significant correlations were considered at *q*-value < 0.01. To compare the inter-specific variability versus inter-specific variability of each trait we calculated the ratio of the corresponding coefficient of variation of standard deviation.

Principal component analyses (PCA) were performed using the function *PCA* of the *FactorMineR* R package . We considered several sets of traits (e.g. all traits, or traits linked to sensitivities to temperature and VPD only), with data at the accession level. Values of each species on the first five axes of the PCA were determined by calculating the barycentre of all accessions in each species. A hierarchical clustering on principal components analysis (HCPC) of species was then performed based on these values on the first five axes of the HCPC using the '*HCPC* function of the *FactorMineR* package. Approximately Unbiased (AU) p-values (%) were calculated with the *pvclust* function from *pv.clust* R package, with 1,000 bootstrap replications.

Results

Inter-specific variability of traits related to plant structure and rates of development, leaf expansion, and transpiration and their response to temperature and vapour pressure deficit

We measured nine traits related to plant structure and three traits related to the rate of plant development and growth in 60 accessions covering a wide genetic diversity in 12 groups (5 accessions in each group) of wheat-related species and subspecies (Fig. 1). Traits related to the rates of plant development and growth (LAR, LERm) and plant size (LA2, LAT, and PN) showed a high variability and significant differences between species (Fig. 3, Supplementary Table S3). Among these traits, LAR increased with ploidy level (Fig. 4l, $P < 10^{-3}$), while LA2, LAT, and PN were higher for the diploid species than for the polyploid species (2n > 4n > 6n; Fig. 4a,d,h, $P < 10^{-3}$ for these three traits). Traits linked to plant structure but expected not to be linked to plant size (i.e. rlw2, rLA, and sLAK) showed no clear patterns with ploidy (Fig. 4b,f,g). The other traits (TL, SLN, and TR) showed less clear pattern. As MLA, SLN showed a low overall variability compared to the other traits we measured.

We analysed the sensitivities of LER to temperature and VPD in the 60 studied accessions. Each night, a temperature between 4°C and 36°C was tested during 6 h after a period of 6 h at the reference temperature of 20°C (Supporting Information Fig. S1). Figure 2 shows an example for *T. turgidum* subsp. *durum*, cultivar Brumaire, where temperature was first maintained at 20°C during 6 h and then increased to 24°C during 6 h. LER oscillated around 4 mm h^{-1} during the first period at 20°C and then increased rapidly to about 5 mm h^{-1} when temperature was increased to 24°C (Fig. 2c). We normalized LER measured at the tested temperature by that measured during the same night at the reference temperature to analyse the effect of temperature change regardless of differences in LER, due to differences in leaf rank or time since leaf emergence (Fig. 4a). We fitted the data to three different function equations to estimate the cardinal temperatures of LER: a beta function , an Arrhenius function , and a segmented linear equation (Eqn 1). For all accessions, the segmented linear model was the best model (Supporting Information Fig. S2 and Table S5). All data were thus analysed using this model. The type of responses we obtained is illustrated in Figure 4a.

The three cardinal temperatures showed a moderate but significant variability between the 12 groups of species and subspecies (Fig. 3), T_{min} ranged from -1.7°C to 3.9°C, T_{opt} from 24.0°C to 31.6°C and T_{max} from 36.2°C to 53.4°C (Supplementary Information Table S6). We observed no clear pattern between ploidy levels, genomes, or between wild versus domesticated species (Fig. 4d-f).

We quantified the responses of LER and TR to VPD during the day using an approach similar to that described above for the response of LER to temperature during the night. VPD in the growth chamber was controlled at 1.3 kPa during the first 6 h of the day, then it was changed between 0.5 and 3.0 kPa until the end of the day. The type of responses we obtained is illustrated in Figure 4b and 4c for LER and TR, respectively. LER oscillated around 5.5 mm h^{-1} at the reference VPD and decreased to 4 mm h^{-1} when VPD was increased to 2.7 kPa. At the same time, TR, which stabilized at 13 g h^{-1} at the reference VPD, increased to 19 g h^{-1}. LER and TR at the tested VPD were normalized by their corresponding value at the reference VPD, removed the effects of leaf rank, time since leaf emergence, and plant leaf area. Both responses to VPD were modelled with a linear model, the slope of which is the response of LER (sLER) or TR (sTR) to VPD (Fig. 4b,c). Both sensitivities showed a significant variability between species and subspecies (Fig. 4g,h), with sTR ranging from -0.268 to -0.037 kPa, and sLER from 0.260 to 0.805 kPa (Supplementary Information Table S6). However, at the level of single traits, we did not observe clear pattern between the 12 groups of species.

Ploidy level, phylogeny, and breeding together explain the phenotypic space of all traits

Apprehending the structure of the interspecific diversity and how the intra-specific diversity is nested inside is possible by considering the n-dimensional space constituted by all traits together (phenotypic space). We found significant correlations between most traits (Fig. 5 and Supporting Information Table S7). The strongest positive correlations were between traits related to plant structure and plant size. However, we also found significant correlations between traits of different types, for example between response traits and traits related to plant structure.

We reduced the dimension of the phenotypic space to five dimensions by using principal component analyses (PCAs). PCA based on all traits at the accession level (Fig. 6a-d) showed that within each group of species, the diversity of values for the three first components was low compared to the overall diversity observed at the interspecific level (Fig. 6b). The first principal component (PC1) explained 30% of the observed variance and was mainly explained by traits related to development rate (e.g. LAR and LERm) and traits linked to plant size (e.g. LAT and TL; Fig. 6a) and discriminated diploid species from tetraploid and hexaploid species (Fig. 6b). Diploid species had smaller leaf 2 (LA2), lower leaf appearance rate (LAR), less leaves (TL) and a lower leaf area (LAT) compared with tetraploid and hexaploid species (Fig. 3). However, because most of the wild species

used in this study are diploids, and because *T. turgidum* subsp. *dicoccoides* was close to the origin of PC1, we cannot conclude if this axis discriminated species based on domestication or ploidy level.

The clustering analysis based on the first five components of the PCA classified the 12 groups into six clusters (Fig. 6e). The first branching of the dendogram (corresponding to the highest relative distance) separated the diploid and polyploid species. For the diploids, the second order of the dendrogram separated the genome A from the other two diploid genomes, and for the polyploidy it separated *T. turgidum* subsp. *dicoccoides* and *T. turgidum* subsp. *dicoccum* from the others polyploid species. The third order of clustering grouped together *T. turgidum* subsp. *durum* elite cultivars and the two hexaploid species (*T. aestivum* subsp. *aestivum* and *T. aestivum* subsp. *spelta*), while *T. turgidum* subsp. *durum* landraces were grouped with *T. turgidum* subsp. *turgidum*. The wild and cultivated emmer wheat species (*T. turgidum* subsp. *dicoccoides* and *T. turgidum* subsp. *dicoccum*) were grouped together. Therefore, the phenotypic space based onb the 17 traits we studied discriminated wheat-related species and subspecies based on their ploidy level, domestication and breeding, and the resulting clustering of species fitted well the phylogeny of the 12 groups of species and subspecies.

Phylogeny structured the phenotypic space of traits related to the rate of plant development and growth and their responses to temperature and vapour pressure deficit

A similar analysis combining PCA and HCA but based on traits linked to plant structure only (Supporting information Fig. S3) showed similar results as that performed on all 17 traits (with marginal differences), suggesting that structure traits drove the clustering of the 12 groups of species. Therefore, we performed a similar analysis on traits linked to rates and sensitivities, and excluding structure traits (Fig. 7).The first axis opposed species with high LAR to species with low TR, sLER and T_{max}, while the second axis opposed species with high T_{max} to species with low T_{min}, T_{opt} and sTR. T_{opt} was negatively correlated with LERm (Supplementary Information Table S7) and were the main contributing traits to the third axis. The resulting HCA first segregated two groups. The first one consisted of the cultivated tetraploid and hexaploid species, as well as *Ae. Tauschii*, while the second one consisted of the wild and cultivated diploids and the wild tetraploid species *T. turgidum* subs. *dicoccoides*. Within these two groups, the HCA produced only few unexpected results : (i) *T. turgidum* subs. *dicoccoides* clustered with *T. monococcum* (subsp. *monococcum* and *beoticum*), (ii) *T. aestivum* subs. *spelta* clustered with a group of three *T. turgidum* and (iii) *Ae. tauschii* was in the same cluster as *T. aestivum* subs. *aestivum.* Overall, these results indicated that the rate of

development of growth and the sensitivities to temperature and VPD are well-conserved, with a low variability within species compared to the phenotypic space of wheat-related species, and that their inter-specific variability is mainly structured by phylogeny.

Finally, we analysed the structure of the phenotypic space of response traits only, knowing that values of individual traits did not show clear trends (Fig. 4). Because the phenotypic space was naturally reduced to five dimensions (five variables), which appeared as independent in a PCA analysis (Fig.8a), we performed aHCA based on these five traits.Here again, clear patterns appeared on the dendogram. The HCA first segregated two wild diploid species *Ae*. *speltoïdes* and *T. uratu from the other species*, indicating that these two wild species had significantly different responses to temperature and evaporative demand compared to the other species. But overall, HCA clustered 3 other groups: (i) one group comprising all tetraploid species, regardless of wild/domesticated subgroups, (ii) one group with the two wild and domesticated *T. monococcum* species, and (iii) one group with the two hexaploid species (*T. aestivum subs spelta* and *aestivum*) and *Ae. Tauschii*, that is, all species with a D genome. This analysis therefore indicated that the inter-specific variability in temperature and VPD responses was structured by both the ploidy level and the phylogenetic relationships. However, domestication and/or breeding pressure does not appear has having modify such responses.

Discussion

Modelling the sensitivities of leaf elongation rate to temperature and vapour pressure deficit and of transpiration rate to vapour pressure deficit for a large genetic diversity in wheat-related species

The response of plant organ expansion processes to temperature has been extensively studied (. Most of these studies concluding in a similar response as that of plant development, and the few studies assessing the intra-specific variability of this response indicated a very low genetic variability within each species (Parent & Tardieu, 2012). It results that most crop models use similar formalisms and parameters values for both the response of development and expansion processes without genetic variability on these parameters (Parent & Tardieu, 2014). Several model formalisms are used in crop models, from the simplest linear model, to more complex curvilinear models . In this study, we used a segmented linear formalism, which adequately fitted to the observed sensitivities in 60 accessions of wheat-related species. As expected, the observed intra-specific variability was low, so

was the inter-specific variability (albeit non-null, see below). It indicates that a modelling strategy based on parsimony; with a single set of parameter values for all wheat-related species was probably a good strategy (Parent et al., 2016). Such a model with no genotypic variation would be probably very close to a model assuming organised genetic variation, but avoiding time consuming experiments on each single wheat accession.

Up to now, to our knowledge, there was no study that assessed the response of leaf elongation to VPD in wheat. However, most cereal species react strongly to changes of evaporative demand and a large genetic variability of the response of LER to VPD has been found in species in which this process has been studied . Here, we show that a linear model can fit this response in a large diversity of wheat-related species. The range of sensitivities at the interspecific level (from -10% to -20% per kPa) was very close to that observed in maize . Because considering this response can greatly improve prediction of leaf area in contrasted field sites in maize, it should also be the case in wheat growth predictions.

While the response of transpiration to VPD has been investigated in many species including bread wheat , and a very high variability was found across generations of selections of Australian wheat , there was no information about its variability in wheat-relative species. Unexpectedly, the variability of responses observed in this study was very low, at both the intra- and inter-specific level compared to that found in 23 cultivars released from 1890 to 2010 in Australia . For some genotypes, Schoppach et al. (2012) observed a break point in the TR-VPD relationship between 2.4 and 3.9 kPa. In the range of VPD we tested, a linear model fitted the response of all accessions without any breakpoint. These results could be explained by the limited range of VPD used here (0.5-3.0 kPa compared with 0.8 to 4.5 kPa in Schoppach et al. (2012)), but which correspond to a physiological range observed in the spring in most temperate regions.

Most traits have probably evolved slowly, following polyploidisation, phylogeny and breeding pressure

A striking result of this study was the fact that a hierarchical clustering of species based on traits that have not been directly selected could reproduce almost perfectly our knowledge about phylogeny of wheat-related species and subspecies. The hierarchical clustering based on traits linked to plant structure discriminated diploid from polyploid species, regardless of domestication (e.g. *T. mococcoccum* subsp. *mococcoccum* and *boeoticum* clustered together and *T. turgidum* subsp. *dicoccoides* and *dicoccum clustered together*). This results suggest a specific effect of ploidy on plant physiology such as that observed in trees . In addition, we found variations depending on the

genome, with different sets of trait values between diploid species with genome A, D or S. Finally, selection pressure seems to have affected these traits (but much less than phylogeny and ploidy), with different clusters of trait values for the earliest tetraploid species (*T. turgidum* subsp. *dicoccoides* and *dicoccum*) and landraces of *T. turgidum* subsp. *durum* selected before the green revolution, compared with later-released durum wheat cultivars.

At the level of individual traits, values of the five traits related to sensitivities to temperature and VPD did not indicate clear patterns, with no obvious impact of selection pressure, domestication, genome or sub-genome, ploidy, or phylogenetic links between species. On the contrary, a clustering based on these traits was showing clear patterns, with an effect of both ploidy and phylogenetic relationships Overall, species that are phylogenetically close showed similar phenotypic spaces, indicating that these traits are well-conserved and have probably evolved slowly, following phylogeny, as proposed earlier for the response to temperature in a much wider genetic diversity of cultivated plants .

Which sources of genetic improvement within species and between related-species?

Our initial intention, in addition to providing formalisms and parameter values for process-based models, was to test the hypothesis that new sources of genetic diversity for the response of LER and TR to VPD and temperature could be found in wheat-related species, in particular in wild or cultivated *T. turgidum* or diploid species, and if this diversity could enrich the genetic diversity of cultivated wheat using a synthetic-wheat strategy .

Most wheat synthetic derived cultivars have been developed by crossing *Ae tauschii* with elite durum wheat cultivars, and more recently *T. dicoccoides, T. dicoccum*, or *T. turgidum* . Several studies have reported significant improvements in heat and drought tolerance of bread wheat cultivars derived from *Ae tauschii* x *T. durum* crosses compared with locally adapted elite cultivars . However, the inter-specific variability of wild and cultivated wheat related species for traits related temperature and evaporative demand has been not explored yet.

As expected, our results showed that the genetic variability of structure traits observed within wheat ancestors or the secondary gene pool is far from that observed in modern durum or bread wheat cultivars but mostly presented lower values, which would not give advantage in agronomical conditions. For these traits, a source of enrichment of genetic diversity should therefore be sought in other wild species. To the contrary, for response traits, some wild relative species or wheat ancestors may provide an adaptive value if introduced in cultivated wheat species.

The response of LER and TR to temperature or VPD in *Ae tauschii* and *T. dicoccum* were similar to those of *T. aestivum*. In particular, accessions of *Ae. tauschii* presented very similar trait values compared to modern wheat lines and they delimitated a phenotypic space that was almost nested in that of *T. aestivum.* In contrast, *T. uratu* and *Ae. speltoïdes* showed very distinct responses and had higher T_{max} and lower sLER than elite bread and durum wheat cultivars. Synthetic tetraploid and hexaploid lines have been created with *T. urartu or Ae. speltoïdes* but, to our knowledge, they have not been evaluated for their response to temperature or evaporative demand . Although the introgression of these species into wheat is practically and methodically more challenging, recent development of genomic resources and biotechnology have good promise to accelerate the use of diploid wheat related species other than *Ae. tauschii* . Several studies therefore focused on the response of vegetative and/or reproductive traits to high temperature in *Aegilops* species, and observed genetic variability at both intra- and inter-specific levels (Pradhan *et al.,* 2012). Although we considered only a very limited number of accessions in each species, our results suggest that *T. urartu and Ae. speltoïdes* could be interesting sources of genes to develop wheat cultivars able to maintain high LER under high temperature and evaporative demand.

Conclusion

In addition to (i) providing new formalisms of trait responses together with model parameters in 12 wheat-related species and subspecies, this study (ii) indicates that traits linked to the responses of LER and TR to temperature and VPD are well-conserved, with an unexpected low genetic variability within species; (iii) that vegetative traits have probably evolved slowly, following phylogenetic links between accessions; (iv) that both domestication and phylogenetic relationships drove the slow evolution of temperature and VPD responses; (v) and identify sources of varietal improvement currently locked in wheat-related species.

Acknowledgement

SL was supported by a Convention Industrielle de Formation par la Recherche (CIFRE convention n° 2017/1069) between ANRT and ITK. The authors thank François Balfourier (UMR GDEC, INRAE, Clermont-Ferrand, France), and Pierre Roumet (UMR AGAP, INRAE, Montpellier, France) for advices for selecting the material and for providing seeds, and Dr. Jacques Le Gouis and Ms. S.Rougeol (UMR GDEC, INRAE, Clermont-Ferrand, France) for genotyping the major genes for the accessions used in this study.

Author contributions

BP and PM designed the research. SL, BP, and PM designed the experiments. SL performed the experiments and SL, BP, and PM analysed the data. BP wrote the first draft. All authors contributed to the revision of the manuscript.

Data availability

The data that support the findings of this study are openly available in "Zenodo" at https://zenodo.org/record/5511805

References

Akaike H. **1974**. A new look at the statistical model identification. IEEE Transactions on Automatic Control **19**: 716–723.

Allahverdiyev TI. **2015**. Physiological Traits of Durum Wheat (Triticum durum Desf.) and Bread Wheat (Triticum aestivum L.) Genotypes under Drought Stress. Agricultural Sciences **06**: 848–859.

Asseng S, Ewert F, Rosenzweig C, Jones JW, Hatfield JL, Ruane AC, Boote KJ, Thorburn PJ, Rötter RP, Cammarano D, et al. 2013. Uncertainty in simulating wheat yields under climate change. Nature Climate Change **3**: 827–832.

Barlow E, Boersma L. **1972**. Growth Response of Corn to Changes in Root Temperature and Soil-Water Suction Measured with an Lvdt. Crop Science **12**: 251-252.

Ben-Ari T, Boe J, Ciais P, Lecerf R, Van der Velde M, Makowski D. **2018**. Causes and implications of the unforeseen 2016 extreme yield loss in the breadbasket of France. Nature Communications **9**: 1627.

Brunazzi A, Scaglione D, Talini RF, Miculan M, Magni F, Poland J, Pè ME, Brandolini A, Dell'Acqua M. **2018**. Molecular diversity and landscape genomics of the crop wild relative Triticum urartu across the Fertile Crescent. The Plant Journal **94**: 670–684.

Comai L. **2005**. The advantages and disadvantages of being polyploid. Nature Reviews Genetics **6**: 836–846.

Davies WJ, Wilkinson S, Loveys B. **2001**. Stomatal control by chemical signalling and the exploitation of this mechanism to increase water use efficiency in agriculture. New Phytologist **153**: 449–460.

De Baerdemaeker NJF, Hias N, Van den Bulcke J, Keulemans W, Steppe K. **2018**. The effect of polyploidization on tree hydraulic functioning. American Journal of Botany **105**: 161–171.

Dejong R, Best K. **1979**. Effect of Soil-Water Potential, Temperature and Seeding Depth on Seedling Emergence of Wheat. Canadian Journal of Soil Science **59**: 259–264.

Gallagher JN, Biscoe PV, Wallace JS. **1979**. Field Studies of Cereal Leaf GrowthIV. WINTER WHEAT LEAF EXTENSION IN RELATION TO TEMPERATURE AND LEAF WATER STATUS. Journal of Experimental Botany **30**: 657–668.

Giunta F, Pruneddu G, Zuddas M, Motzo R. **2019**. Bread and durum wheat: Intra- and inter-specific variation in grain yield and protein concentration of modern Italian cultivars. European Journal of Agronomy **105**: 119–128.

Hammer G, Messina C, Wu A, Cooper M. **2019**. Biological reality and parsimony in crop models—why we need both in crop improvement! in silico Plants **1**: diz010.

Handmer J, Honda Y, Kundzewicz ZW, Arnell N, Benito G, Hatfield J, Mohamed IF, Peduzzi P, Wu S, Sherstyukov B, et al. 2012. Changes in Impacts of Climate Extremes: Human Systems and Ecosystems (CB Field, V Barros, TF Stocker, Q Dahe, DJ Dokken, KL Ebi, MD Mastrandrea, KJ Mach, GK Plattner, SK Allen, et al., Eds.). Cambridge: Cambridge Univ Press.

Haun JR. **1973**. Visual Quantification of Wheat Development1. Agronomy Journal **65**: 116.

Hias N, Svara A, Keulemans JW. **2018**. Effect of polyploidisation on the response of apple (Malus × domestica Borkh.) to Venturia inaequalis infection. European Journal of Plant Pathology **151**: 515–526.

Jeuffroy M-H, Casadebaig P, Debaeke P, Loyce C, Meynard J-M. **2014**. Agronomic model uses to predict cultivar performance in various environments and cropping systems. A review. Agronomy for Sustainable Development **34**: 121–137.

Josephides CM. **1992**. Analysis of adaptation of barley, triticale, durum and bread wheat under Mediterranean conditions. Euphytica **65**: 1–8.

Kemp D, Blacklow W. **1982**. The Responsiveness to Temperature of the Extension Rates of Leaves of Wheat Growing in the Field Under Different Levels of Nitrogen-Fertilizer. Journal of Experimental Botany **33**: 29–36.

Kishii M. **2019**. An Update of Recent Use of Aegilops Species in Wheat Breeding. Frontiers in Plant Science **10**.

Kumudini S, Andrade FH, Boote KJ, Brown GA, Dzotsi KA, Edmeades GO, Gocken T, Goodwin M, Halter AL, Hammer GL, et al. 2014. Predicting Maize Phenology: Intercomparison of Functions for Developmental Response to Temperature. Agronomy Journal **106**: 2087–2097.

Lacube S, Fournier C, Palaffre C, Millet EJ, Tardieu F, Parent B. **2017**. Distinct controls of leaf widening and elongation by light and evaporative demand in maize. Plant Cell and Environment **40**: 2017–2028.

Lê S, Josse J, Husson F. **2008**. FactoMineR: A Package for Multivariate Analysis. Journal of Statistical Software **25**: 1–18.

Li A, Liu D, Yang W, Kishii M, Mao L. **2018**. Synthetic Hexaploid Wheat: Yesterday, Today, and Tomorrow. Engineering **4**: 552–558.

Lobell DB, Schlenker W, Costa-Roberts J. **2011**. Climate Trends and Global Crop Production Since 1980. Science **333**: 616–620.

Lopes MS, Reynolds MP. **2011**. Drought Adaptive Traits and Wide Adaptation in Elite Lines Derived from Resynthesized Hexaploid Wheat. Crop Science **51**: 1617–1626.

López-Castañeda C, Richards RA. **1994**. Variation in temperate cereals in rainfed environments I. Grain yield, biomass and agronomic characteristics. Field Crops Research **37**: 51–62.

Mariano Cossani C, Reynolds MP. **2015**. Heat Stress Adaptation in Elite Lines Derived from Synthetic Hexaploid Wheat. Crop Science **55**: 2719–2735.

Marti J, Slafer GA. **2014**. Bread and durum wheat yields under a wide range of environmental conditions. Field Crops Research **156**: 258–271.

Martin A, Simpfendorfer S, Hare RA, Eberhard FS, Sutherland MW. **2011**. Retention of D genome chromosomes in pentaploid wheat crosses. Heredity **107**: 315–319.

Monneveux P, Jing R, Misra SC. **2012**. Phenotyping for drought adaptation in wheat using physiological traits. Frontiers in Physiology **3**.

Parent B, Millet EJ, Tardieu F. **2019**. The use of thermal time in plant studies has a sound theoretical basis provided that confounding effects are avoided. Journal of Experimental Botany **70**: 2359–2370.

Parent B, Suard B, Serraj R, Tardieu F. **2010a**. Rice leaf growth and water potential are resilient to evaporative demand and soil water deficit once the effects of root system are neutralized. Plant, Cell & Environment **33**: 1256–1267.

Parent B, Tardieu F. **2012**. Temperature responses of developmental processes have not been affected by breeding in different ecological areas for 17 crop species. New Phytologist **194**: 760–774.

Parent B, Tardieu F. **2014**. Can current crop models be used in the phenotyping era for predicting the genetic variability of yield of plants subjected to drought or high temperature? Journal of Experimental Botany **65**: 6179–6189.

Parent B, Turc O, Gibon Y, Stitt M, Tardieu F. **2010b**. Modelling temperature-compensated physiological rates, based on the coordination of responses to temperature of developmental processes. Journal of Experimental Botany: erq003.

Perego A, Sanna M, Giussani A, Chiodini ME, Fumagalli M, Pilu SR, Bindi M, Moriondo M, Acutis M. **2014**. Designing a high-yielding maize ideotype for a changing climate in Lombardy plain (northern Italy). Science of the Total Environment **499**: 497–509.

Petersen G, Seberg O, Yde M, Berthelsen K. **2006**. Phylogenetic relationships of Triticum and Aegilops and evidence for the origin of the A, B, and D genomes of common wheat (Triticum aestivum). Molecular Phylogenetics and Evolution **39**: 70–82.

Pradhan GP, Prasad PVV, Fritz AK, Kirkham MB, Gill BS. 2012. High Temperature Tolerance in Aegilops Species and Its Potential Transfer to Wheat. Crop Sci. **52**: 292–304

R Core Team. **2018**. R: A Language and Environment for Statistical Computing. Vienna, Austria: R Foundation for Statistical Computing.

Rebetzke GJ, Botwright TL, Moore CS, Richards RA, Condon AG. **2004**. Genotypic variation in specific leaf area for genetic improvement of early vigour in wheat. Field Crops Research **88**: 179–189.

Reyer CPO, Leuzinger S, Rammig A, Wolf A, Bartholomeus RP, Bonfante A, de Lorenzi F, Dury M, Gloning P, Abou Jaoude R, et al. 2013. A plant's perspective of extremes: terrestrial plant responses to changing climatic variability. Global Change Biology **19**: 75–89.

Rojas M, Lambert F, Ramirez-Villegas J, Challinor AJ. **2019**. Emergence of robust precipitation changes across crop production areas in the 21st century. Proceedings of the National Academy of Sciences of the United States of America **116**: 6673–6678.

Rosyara U, Kishii M, Payne T, Sansaloni CP, Singh RP, Braun H-J, Dreisigacker S. **2019**. Genetic Contribution of Synthetic Hexaploid Wheat to CIMMYT's Spring Bread Wheat Breeding Germplasm. Scientific reports **9**: 12355–12355.

Rotter RP, Tao F, Hohn JG, Palosuo T. **2015**. Use of crop simulation modelling to aid ideotype design of future cereal cultivars. Journal of Experimental Botany **66**: 3463–3476.

Schoenfelder KP, Fox DT. **2015**. The expanding implications of polyploidy. The Journal of Cell Biology **209**: 485–491.

Schoppach R, Fleury D, Sinclair TR, Sadok W. **2017**. Transpiration Sensitivity to Evaporative Demand Across 120 Years of Breeding of Australian Wheat Cultivars. Journal of Agronomy and Crop Science **203**: 219–226.

Schoppach R, Sadok W. **2012**. Differential sensitivities of transpiration to evaporative demand and soil water deficit among wheat elite cultivars indicate different strategies for drought tolerance. Environmental and Experimental Botany **84**: 1–10.

Schoppach R, Taylor JD, Majerus E, Claverie E, Baumann U, Suchecki R, Fleury D, Sadok W. **2016**. High resolution mapping of traits related to whole-plant transpiration under increasing evaporative demand in wheat. Journal of Experimental Botany **67**: 2847–2860.

Schwarz G. **1978**. Estimating the Dimension of a Model. The Annals of Statistics **6**: 461–464.

Singh RP, Trethowan R. **2008**. Breeding Spring Bread Wheat for Irrigated and Rainfed Production Systems of the Developing World. In: Breeding Major Food Staples. John Wiley & Sons, Ltd, 107–140.

Tardieu F. **2012**. Any trait or trait-related allele can confer drought tolerance: just design the right drought scenario. Journal of Experimental Botany **63**: 25–31.

Tardieu F, Parent B. **2017**. Predictable 'meta-mechanisms' emerge from feedbacks between transpiration and plant growth and cannot be simply deduced from short-term mechanisms. Plant, Cell & Environment **40**: 846–857.

Tardieu F, Parent B, Caldeira CF, Welcker C. **2014**. Genetic and physiological controls of growth under water deficit. Plant Physiology: pp.113.233353.

Tu Y, Jiang A, Gan L, Hossain M, Zhang J, Peng B, Xiong Y, Song Z, Cai D, Xu W, et al. 2014. Genome duplication improves rice root resistance to salt stress. Rice **7**.

Valkoun JJ. **2001**. Wheat pre-breeding using wild progenitors. Euphytica **119**: 17–23.

Wang E, Engel T. **1998**. Simulation of phenological development of wheat crops. Agricultural Systems **58**: 1–24.

Wang E, Martre P, Zhao Z, Ewert F, Maiorano A, Rötter RP, Kimball BA, Ottman MJ, Wall GW, White JW, et al. 2017. The uncertainty of crop yield projections is reduced by improved temperature response functions. Nature Plants **3**: 1–13.

Welcker C, Sadok W, Dignat G, Renault M, Salvi S, Charcosset A, Tardieu F. **2011**. A Common Genetic Determinism for Sensitivities to Soil Water Deficit and Evaporative Demand: Meta-Analysis of Quantitative Trait Loci and Introgression Lines of Maize. Plant Physiology **157**: 718–729.

Tables

Table 1. Symbol, units and definition of the structural, rate and response phenotypic trait measured in this study.

Trait type	Symbol	Units	Definition
Structural	LA2	cm^2	Leaf area of leaf 2
	rlw2	-	Ratio length / width for leaf 2
	TL	Leaf $plant^{-1}$	Total number of leaves per plant (main stem + tillers)
	LAT	cm^2 (leaf) $plant^{-1}$	Leaf area per plant (sheath + leaf blade)
	MLA	g m^{-2}	Specific leaf mass
	r_{LA}	-	Ratio of sheath to blade leaf area
	s_{LAK}	-	Slope of the relationship between individual leaf area and leaf rank normalized by the leaf area of leaf 2
	PN	g N $plant^{-1}$	Shoot nitrogen mass
	SLN	g N m^{-2}	Specific leaf (sheath + blade) nitrogen
Rates	LERm	mm h^{-1}	Maximal elongation rate of leaf 5 at 20°C and 1.0 kPa
	TR	g H_20 h^{-1} m^{-2}	Plant transpiration rate at 20°C and 1.3 kPa
	LAR	leaf °C d^{-1}	Average leaf appearance rate
Responses	T_{min}	°C	Minimum temperature for leaf elongation
	T_{opt}	°C	Optimum temperature for leaf elongation
	T_{max}	°C	Maximum temperature for leaf elongation
	s_{LER}	kPa^{-1}	Response of leaf elongation rate to vapour pressure deficit
	s_{TR}	kPa^{-1}	Response of transpiration rate to vapour pressure deficit

Figure legends

Fig. 1 The evolutionary and genome relationships between cultivated wheat species and related wild species used in this study. The origin of B genome is still unclear but it comes from an *Ae.* Sect. *Sitopisis*, represented here by *Ae. speltoides. T. turgidum* subsp. *durum* was separated in two groups: landrace populations grown before the green revolution and elite cultivars released after the green revolution.

Fig. 2 Time courses of air temperature (a), air VPD (b), leaf elongation rate, and transpiration rate during the third night and day of scenario 1. Vertical grey lines indicate the 4-h periods during which environmental conditions were considered stable and leaf elongation rate and transpiration rate were averaged (black lines). In (c) and (d) data are for *T. turgidum* subsp. *durum*, cultivar Brumaire. All measurement were performed on the same plant.

Fig. 3 Traits related to plant structure and rate of development, leaf expansion and transpiration for the 12 groups of wheat related species and subspecies. (a) LAR, leaf appearance rate; (b) LERm, leaf elongation rate of leaf 5 at 20°C and 1.0 kPa; (c) TR, transpiration rate at 20°C and 1.3 kPa; (d) TL, total number of leaves per plant; (e) LAT, leaf surface area per plant; (f) LA2, surface area of leaf 2; (g) rlw2, length-to-width ratio of leaf 2; (h) rLA, ratio of leaf blade to total leaf surface area; (i) sLAK, slope of normalized leaf blade surface area versus leaf rank normalized by the surface area of leaf 2; (j) PN, total N mass per plant; (k) MLA, specific leaf mass; (l) SLN, specific leaf mass. Data are mean ± 1 s.d. for n = 5 accessions.

Fig. 4 Response of leaf elongation rate (LER) to temperature and vapour pressure deficit (VPD), and response of transpiration rate (TR) to VPD for wheat related species and subspecies. (a) and (b) normalized LER versus leaf-air VPD and temperature of the leaf growth zone for *T. turgidum* subsp. *durum* cultivar Neodur, respectively. Data are mean ± 1 s.d. for n = 6 independent replicates for temperatures between 12°C and 28°C and for n =3 for the other temperatures. (c) Normalized TR versus leaf-air VPD for *T. turgidum* subsp. *durum* cultivar Neodur. Data are mean ± 1 s.d. for n = *6* independent replicates. In (a) to (c), black lines are linear (a and c) and segmented-linear (c)

regressions, and horizontal and vertical grey lines indicate the normalization point constraining the fitted function equations. (d), (e), and (f) minimum (T_{min}), optimum (T_{opt}), and maximum (T_{max}) temperature of the leaf meristematic zone for LER, for the 12 groups of wheat-related species and subspecies, respectively. (g) and (h) response of LER (sLER) and transpiration rate (sTR) to leaf-air VPD for the 12 groups of wheat-related species and subspecies. In (d) to (h) data are mean ± 1 s.d. for n = 5 accessions.

Fig. 5 Correlograms of Spearman's correlation coefficients between traits at the accession level (see Table 1 for definitions of variables). (a) Positive correlations. (b) Negative correlations. Traits in blue font are related to plant structure, those in yellow font to absolute rates of development, expansion or transpiration, and those in red font to the response of LER to temperature and VPD and of TR to VPD. Thickness and colour of lines indicate the correlation coefficient value. Only significant (q-value < 0.01) correlations are shown.

Fig. 6 Principal component analysis (PCA) and hierarchical clustering on principal components analysis (HCPC) for the 17 traits measured for the 60 studied accessions of wheat related species and subspecies. (a) and (b) Representation of the structural traits (blue), absolute rates of development, expansion, or TR (green), and response of LER to temperature and VPD and of TR to VPD (red) in the PC1-PC2 and PC1-PC3 plans, respectively. (c) and (d) factor maps of the accessions and the barycentre of each cluster identified by the HCPC analysis on the same plans as in (a) and (b), respectively. (e) Dendrogram of the HCPC analysis performed on the barycentre of each species in the first five axes of the PCA. Dashed vertical line shows the threshold of relative distance for clustering species. Number display the Approximately Unbiased (AU) p-value obtained from 1000 bootstrap replications.

Fig. 7 Principal component analysis (PCA) and hierarchical clustering on principal components analysis (HCPC) for the traits related to the absolute rates of development, expansion and transpiration, and response to temperature and VPD for the 60 studied accessions of wheat related species and subspecies. (a) and (b) Representation of absolute rates of development, expansion, or TR (green) and response of LER to temperature and VPD and TR to VPD (red) in the PC1-PC2 and PC1-PC3 plans, respectively. (c) and (d) factor maps of the accessions and the barycentre of each cluster identified by the HCPC analysis on the same plans as in (a) and (b), respectively. (e)

Dendrogram of the HCPC analysis performed on the barycentre of each species in the first five axes of the PCA. Dashed vertical line shows the threshold of relative distance for clustering species. Number display the Approximately Unbiased (AU) p-value obtained from 1000 bootstrap replications.

Fig. 8 Principal component analysis (PCA) and hierarchical clustering based on trait values related to response to temperature and VPD for the 60 studied accessions of wheat related species and subspecies. (a) and (b) Representation of the response of LER to temperature and VPD and TR to VPD (red) in the PC1-PC2 and PC1-PC3 plans, respectively. (c) and (d) Factor maps of the accessions and the barycentre of each cluster identified by the HCPC analysis on the same plans as in (a) and (b), respectively. (e) Dendrogram of the HCPC analysis performed on the barycentre of each species in the five variables. Dashed vertical line shows the threshold of relative distance for clustering species. Number display the Approximately Unbiased (AU) p-value obtained from 1000 bootstrap replications.

Figure 1

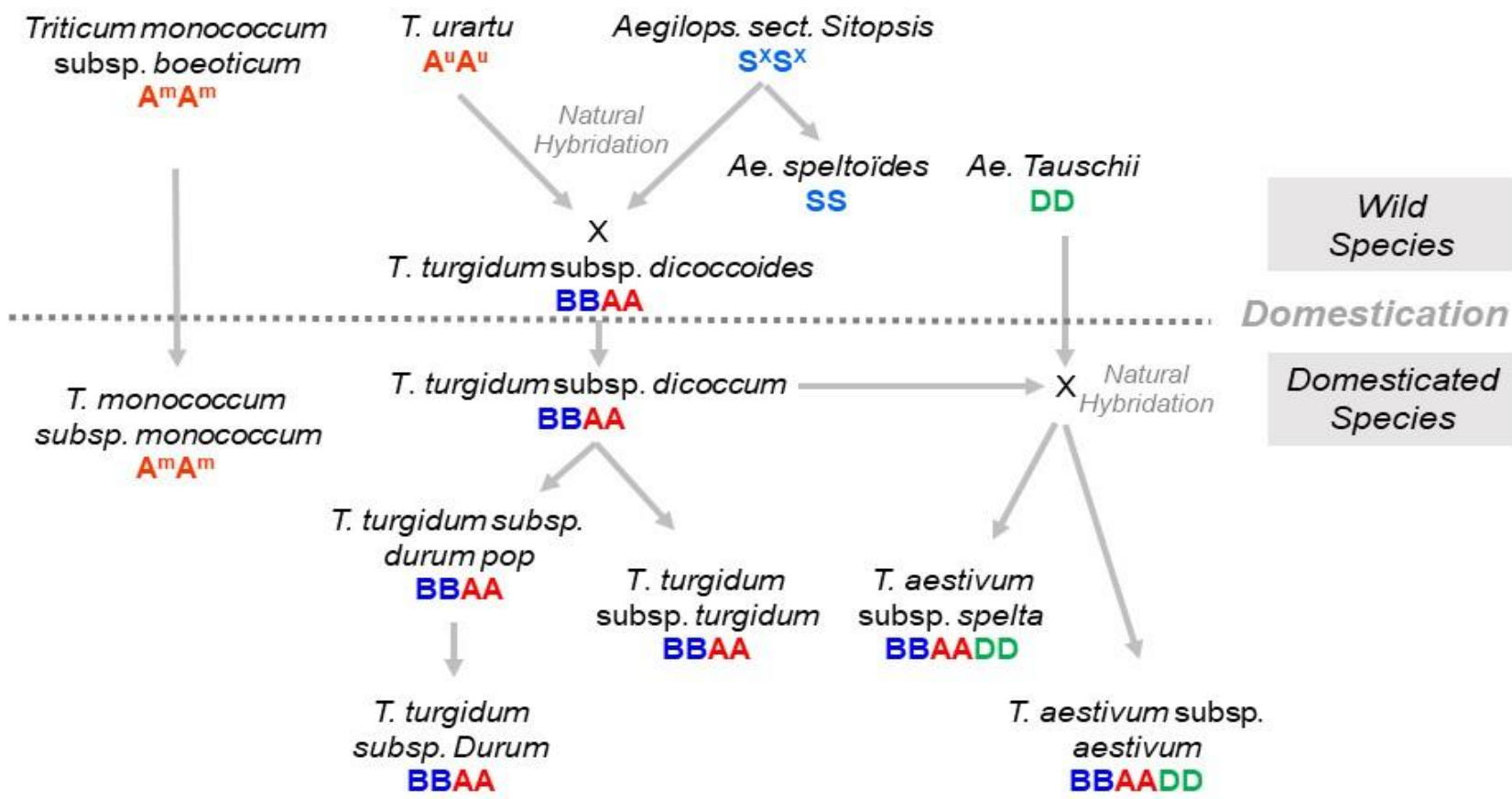

Fig. 1 The evolutionary and genome relationships between cultivated wheat species and related wild species used in this study. The origin of B genome is still unclear but it comes from an *Ae.* Sect. *Sitopisis*, represented here by *Ae. speltoides. T. turgidum* subsp. *durum* was separated in two groups: landrace populations grown before the green revolution and elite cultivars released after the green revolution.

Figure 2

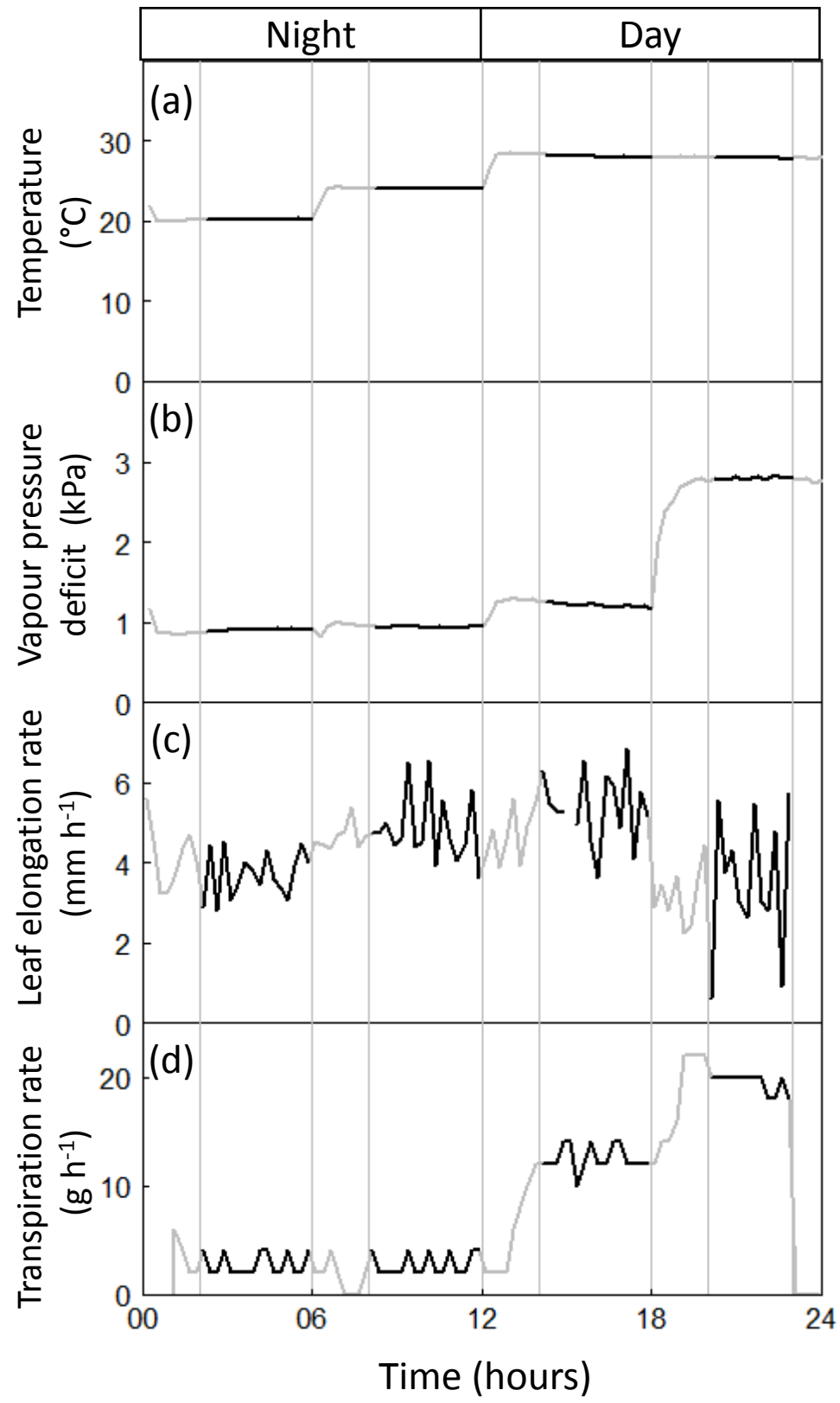

Fig. 2 Time courses of air temperature (a), air VPD (b), leaf elongation rate, and transpiration rate during the third night and day of scenario 1. Vertical grey lines indicate the 4-h periods during which environmental conditions were considered stable and leaf elongation rate and transpiration rate were averaged (black lines). In (c) and (d) data are for T. turgidum subsp. durum, cultivar Brumaire. All measurement were done on the same plant.

Figure 3

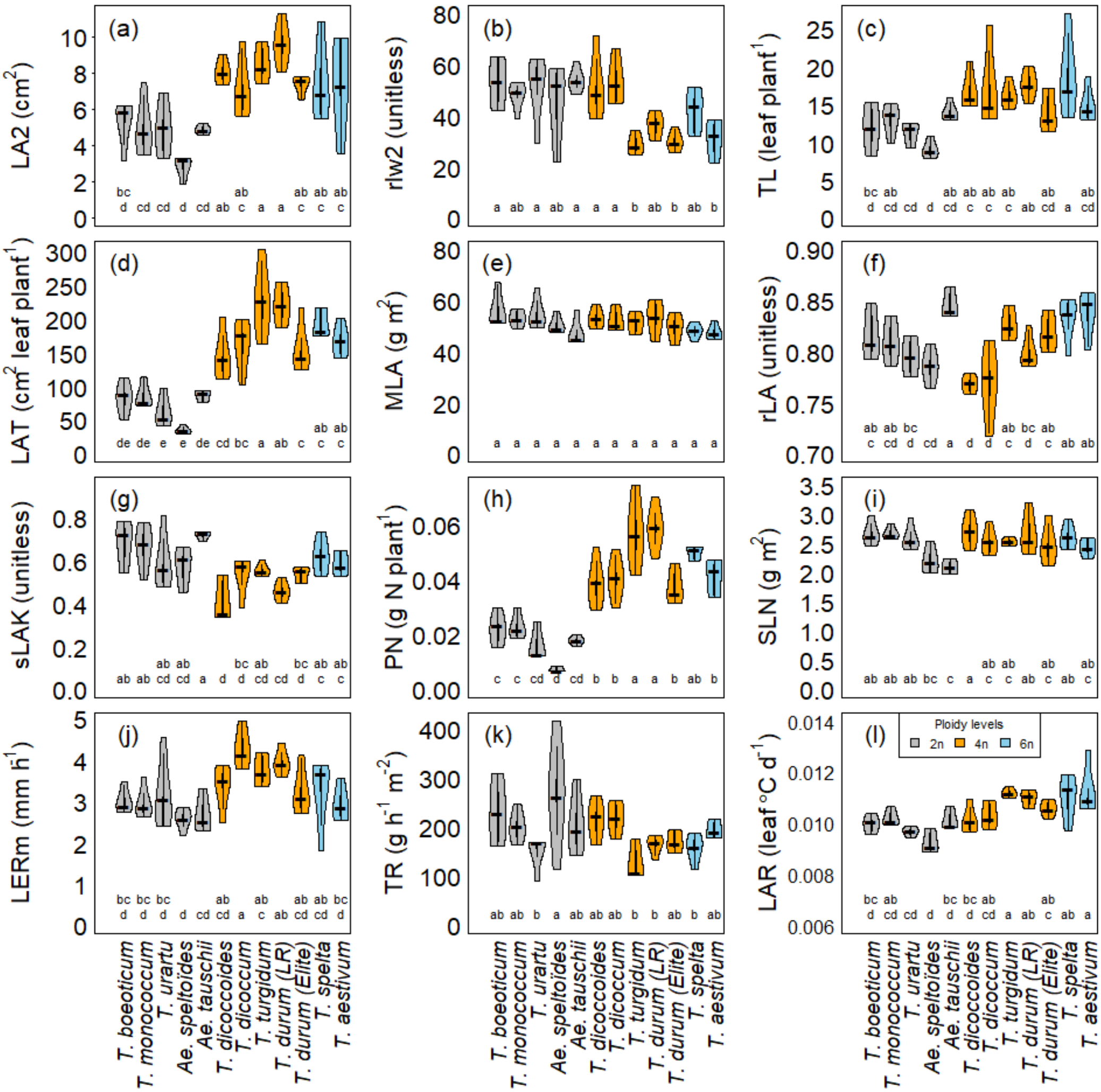

Fig. 3 Traits related to plant structure and rate of development, leaf expansion and transpiration for the 12 groups of wheat related species and subspecies. (a) LA2, surface area of leaf 2; (b) rlw2, length-to-width ratio of leaf 2; (c) TL, total number of leaves per plant; (d) LAT, leaf surface area per plant; (e) MLA, specific leaf mass; (f) rLA, ratio of leaf blade to total leaf surface area; (g) sLAK, slope of normalized leaf blade surface area versus leaf rank normalized by the surface area of leaf 2; (h) PN, total N mass per plant; (i) SLN, specific leaf mass; (j) LERm, leaf elongation rate of leaf 5 at 20°C and 1.25 kPa; (k) TR, transpiration rate at 20°C and 1.25 kPa; (l) LAR, leaf appearance rate. Data are mean ± 1 s.d. for *n* = 5 accessions.

Figure 4

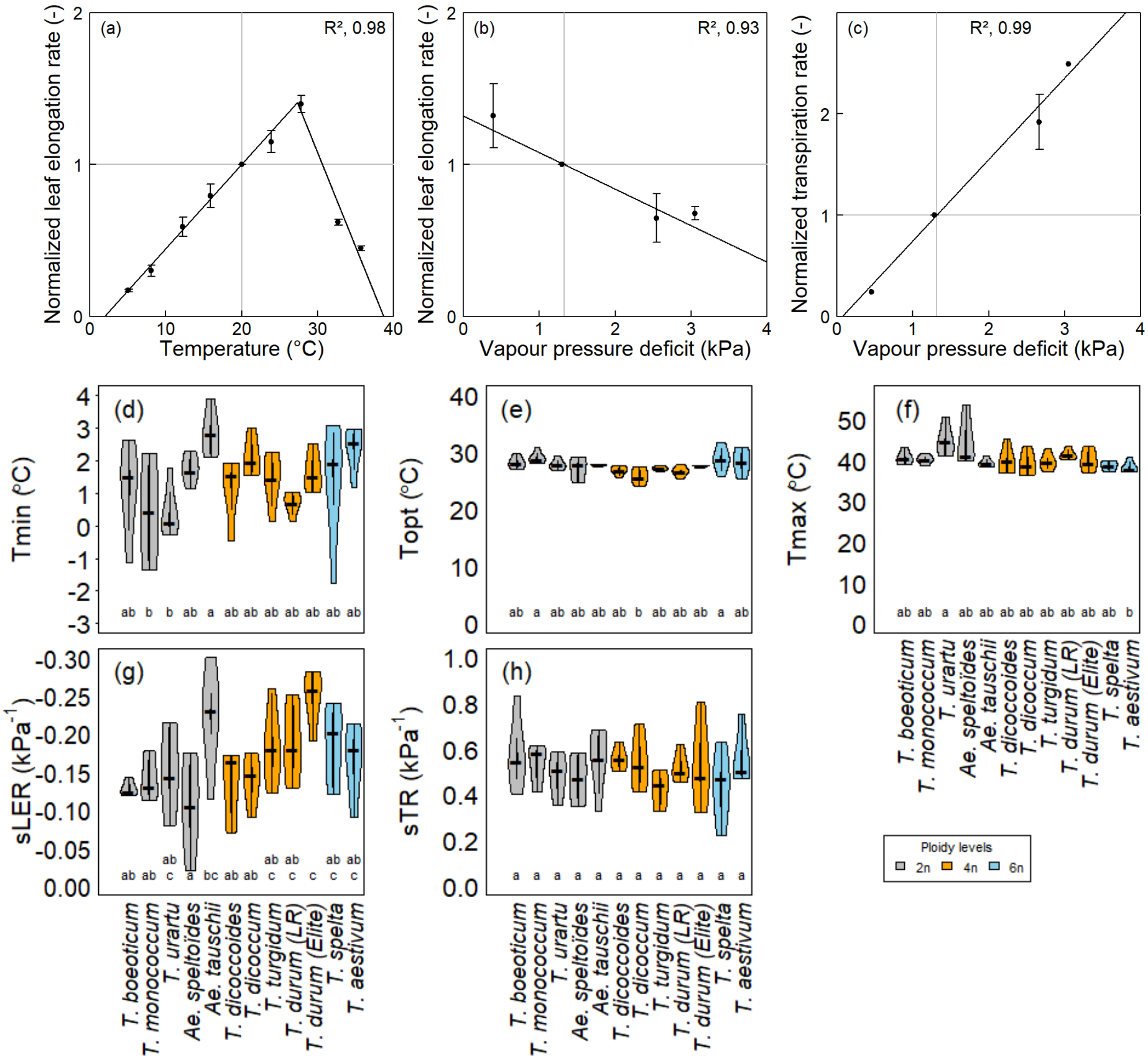

Fig. 4 Response of leaf elongation rate (LER) to temperature and vapour pressure deficit (VPD), and response of transpiration rate (TR) to VPD for wheat related species and subspecies. (a) and (b) normalized LER versus leaf-air VPD and temperature of the leaf growth zone for *T. turgidum* subsp. *durum* cultivar Neodur, respectively. Data are mean ± 1 s.d. for n = 6 independent replicates for temperatures between 12°C and 28°C and for n =3 for the other temperatures. (c) Normalized TR versus leaf-air VPD for *T. turgidum* subsp. *durum* cultivar Neodur. Data are mean ± 1 s.d. for n = *6* independent replicates. In (a) to (c), black lines are linear (a and c) and segmented-linear (c) regressions, and horizontal and vertical grey lines indicate the normalization point constraining the fitted function equations. (d), (e), and (f) minimum (T_{min}), optimum (T_{opt}), and maximum (T_{max}) temperature of the leaf meristematic zone for LER, for the 12 groups of wheat-related species and subspecies, respectively. (g) and (h) response of LER (sLER) and transpiration rate (sTR) to leaf-air VPD for the 12 groups of wheat-related species and subspecies. In (d) to (h) data are mean ± 1 s.d. for n = 5 accessions.

Figure 5

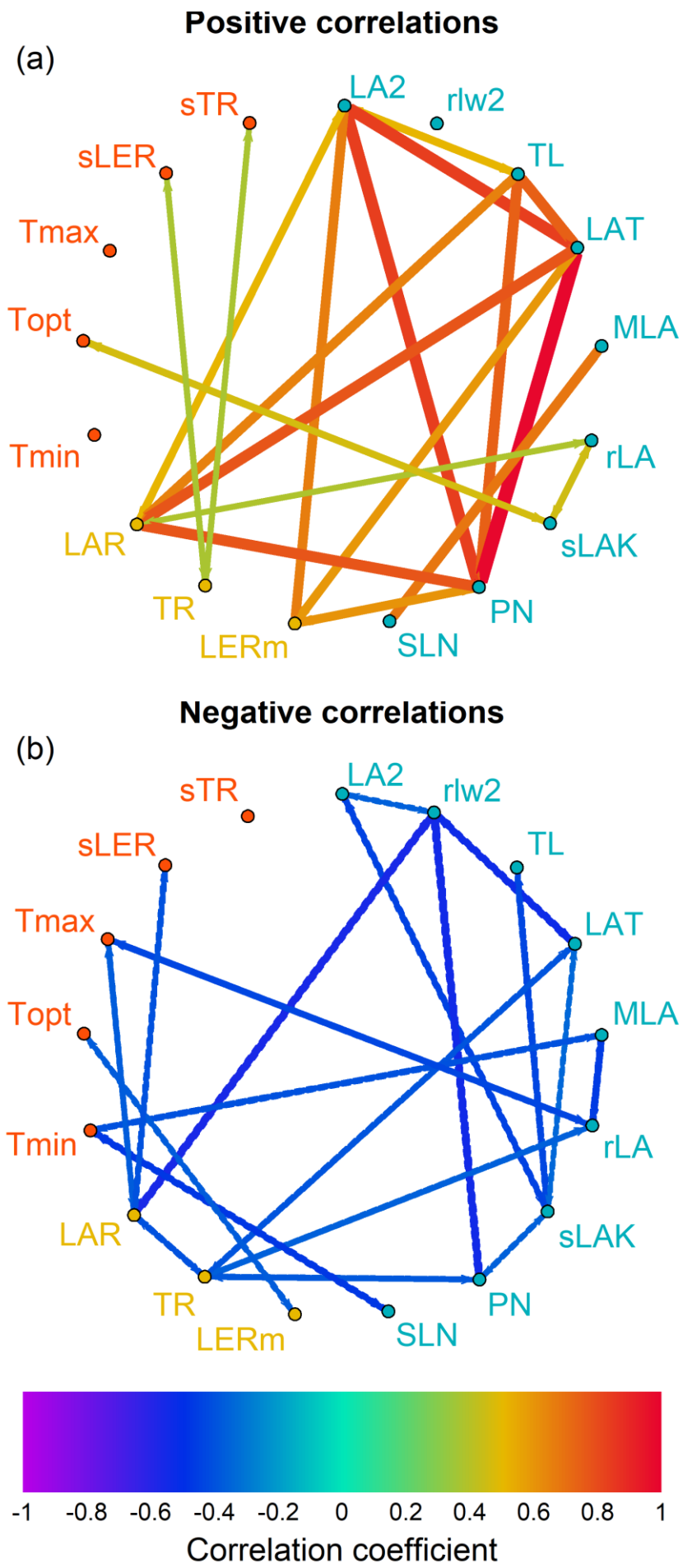

Fig. 5 Correlograms of Spearman's correlation coefficients between traits at the accession level (see Table 1 for definitions of variables). (a) Positive correlations. (b) Negative correlations. Traits in blue font are related to plant structure, those in yellow font to absolute rates of development, expansion or transpiration, and those in red font to the response of LER to temperature and VPD and of TR to VPD. Thickness and colour of lines indicate the correlation coefficient value. Only significant (q-value < 0.01) correlations are shown.

Figure 6

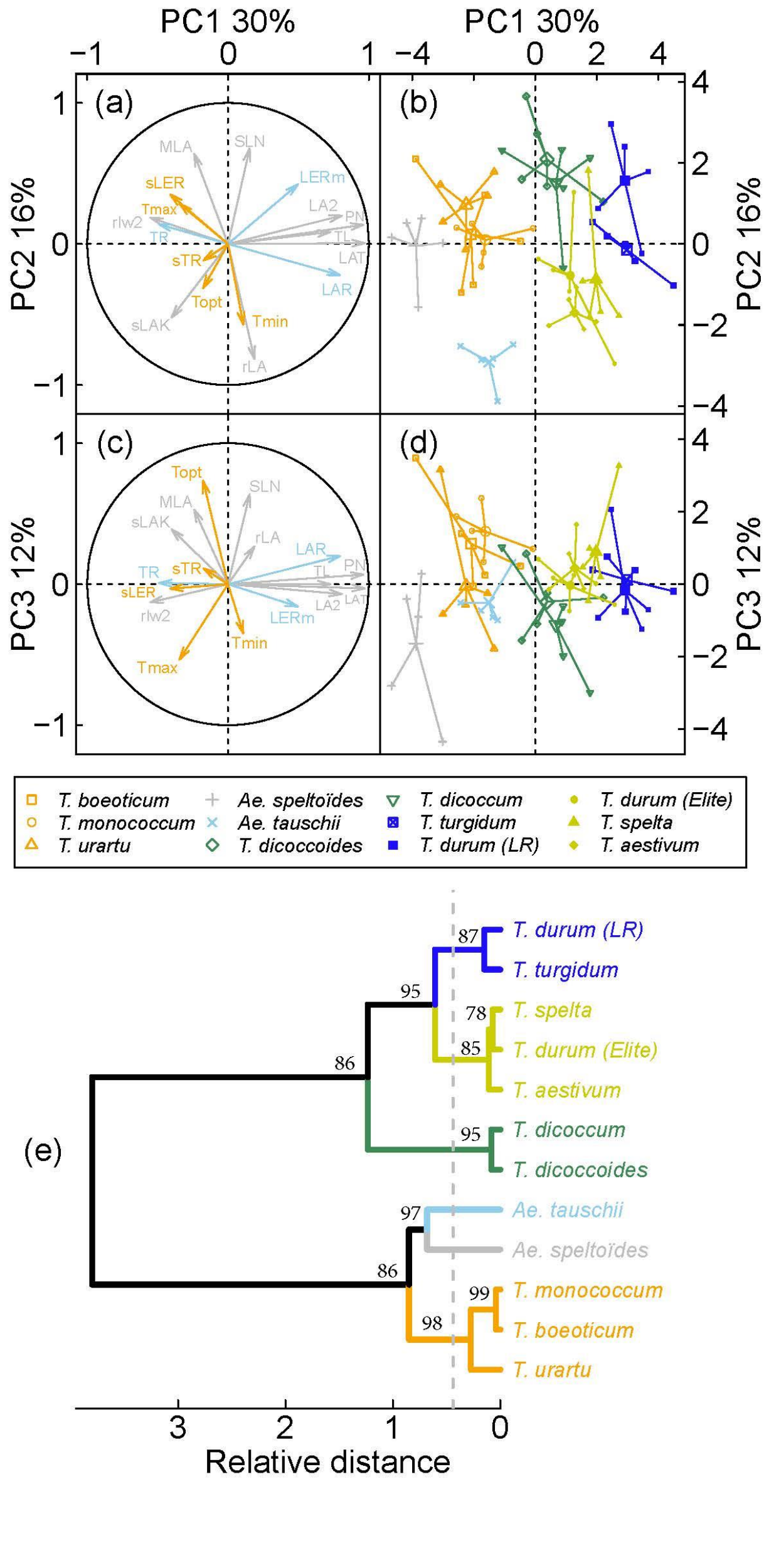

Fig. 6 Principal component analysis (PCA) and hierarchical clustering on principal components analysis (HCPC) for the 17 traits measured for the 60 studied accessions of wheat related species and subspecies. (a) and (b) Representation of the structural traits (blue), absolute rates of development, expansion, or TR (yellow), and response of LER to temperature and VPD and of TR to VPD (red) in the PC1-PC2 and PC1-PC3 plans, respectively. (c) and (d) factor maps of the accessions and the barycentre of each cluster identified by the HCPC analysis on the same plans as in (a) and (b), respectively. (e) Dendrogram of the HCPC analysis performed on the barycentre of each species in the first five axes of the PCA. Dashed vertical line shows the threshold of relative distance for clustering species.

Figure 7

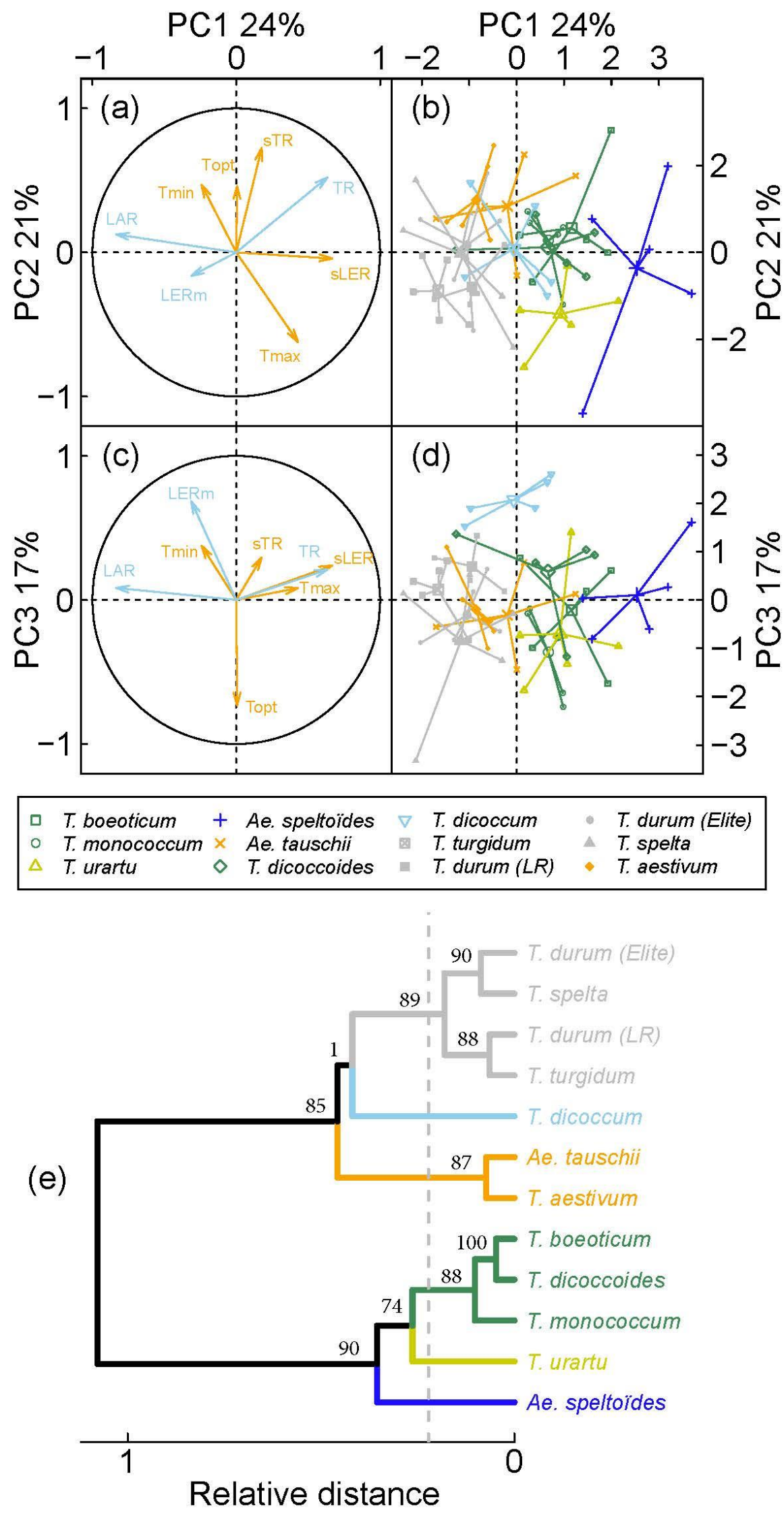

Fig. 7 Principal component analysis (PCA) and hierarchical clustering on principal components analysis (HCPC) for the traits related to the absolute rates of development, expansion and transpiration, and response to temperature and VPD for the 60 studied accessions of wheat related species and subspecies. (a) and (b) Representation of the structural traits (blue), absolute rates of development, expansion, or TR (yellow) and response of LER to temperature and VPD and TR to VPD (red) in the PC1-PC2 and PC1-PC3 plans, respectively. (c) and (d) factor maps of the accessions and the barycentre of each cluster identified by the HCPC analysis on the same plans as in (a) and (b), respectively. (e) Dendrogram of the HCPC analysis performed on the barycentre of each species in the first five axes of the PCA. Dashed vertical line shows the threshold of relative distance for clustering species.

Figure 8

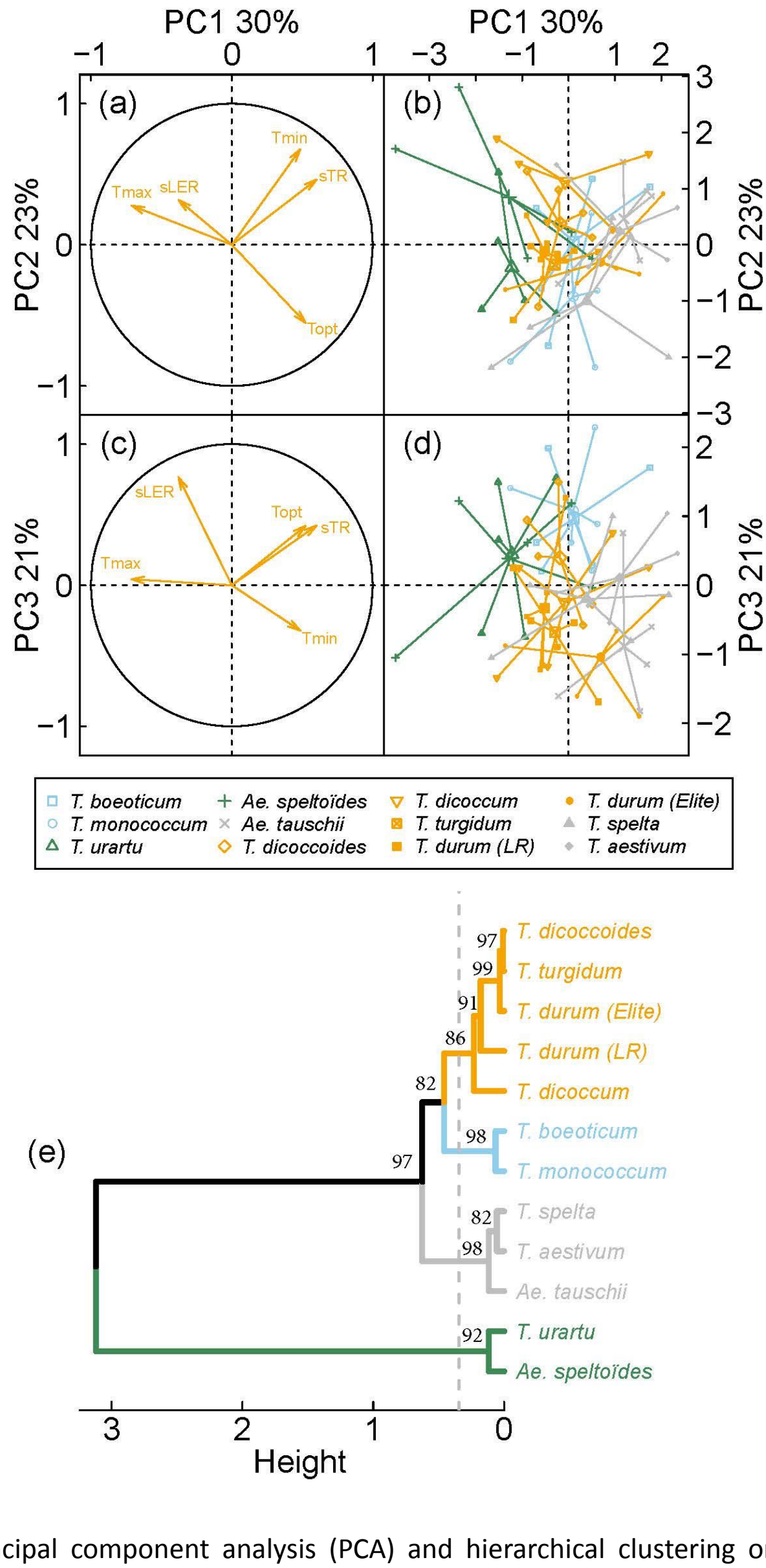

Fig. 8 Principal component analysis (PCA) and hierarchical clustering on principal components analysis (HCPC) for the traits related to response to temperature and VPD for the 60 studied accessions of wheat related species and subspecies. (a) and (b) Representation of the structural traits (blue), absolute rates of development, expansion, or TR (yellow) and response of LER to temperature and VPD and TR to VPD (red) in the PC1-PC2 and PC1-PC3 plans, respectively. (c) and (d) Factor maps of the accessions and the barycentre of each cluster identified by the HCPC analysis on the same plans as in (a) and (b), respectively. (e) Dendrogram of the HCPC analysis performed on the barycentre of each species in the first five axes of the PCA. Dashed vertical line shows the threshold of relative distance for clustering species.